Phase Equilibrium Behavior of the Binary Systems CO_2 + Nonadecane and CO_2 + Soysolv and the Ternary System CO_2 + Soysolv + Quaternary Ammonium Chloride Surfactant

Mohamed M. Elbaccouch,[†] Valeriy I. Bondar,[‡] Ruben G. Carbonell,* and Christine S. Grant

Box 7905−ChE Department, North Carolina State University, Raleigh, North Carolina 27695−7905

Liquid phase and molar volume data were measured for the binary system CO_2 + soysolv at (298.15, 313.15, 323.15, 333.15, and 343.15) K and the ternary system CO_2 + soysolv + quaternary ammonium chloride surfactant at (298.15, 313.15, and 333.15) K, where the composition of soysolv to the surfactant is 99:1 wt % and 80:20 wt % on a CO_2-free basis. Data were collected stoichiometrically with a high-pressure Pyrex glass cell, where no sampling or chromatographic equipment is required. The accuracy of the experimental apparatus was tested with phase equilibrium measurements for the system CO_2 + nonadecane at 313.15 K. A pressure-decay technique was used to calculate the mass of CO_2 loaded into the equilibrium section of the apparatus, and its accuracy was verified with a blank nitrogen experiment. The generated data show that CO_2 modified soysolv is an effective transport medium for the quaternary ammonium chloride surfactant.

Introduction

Understanding the effects of gas solubility and swollen volume on the phase behavior of a mixture is important in various thermodynamic and industrial applications. The feasibility of using CO_2, modified with a food grade oil cosolvent, as an extraction medium for particular compounds in chemical processes is of industrial interest. CO_2 has been receiving industrial attention due to its solvating power, which can be altered dramatically by a slight change in temperature or pressure.[1] In addition, CO_2 is a benign solvent, inexpensive, recyclable, nontoxic, and not flammable.[2] Quaternary ammonium chloride surfactant (BTC 1010-80) is being used in the regeneration of a specific packed ion exchange bed in aqueous media.[3] It is desirable to be able to recycle the surfactant and reduce its waste volume by transporting it with CO_2. The surfactant and CO_2 are not miscible, but the addition of soysolv as a cosolvent to CO_2 can provide the necessary solubility enhancement for removing the surfactant from the slurry after the regeneration process. In this study, solubility data for the binary system CO_2 + soysolv and the ternary system CO_2 + soysolv + quaternary ammonium chloride surfactant were measured.

The quaternary ammonium chloride surfactant contains 80 wt % didecyldimethylammonium chloride, 12 wt % ethanol, and 8 wt % water. The ethanol and water are stabilizing agents for the didecyldimethylammonium chloride to prevent precipitation. The chemical structure of didecyldimethylammonium chloride is given in Figure 1. The quaternary ammonium chloride surfactant has been used industrially in disinfectant, sanitizer, and fungicidal products for hard surfaces in hospitals and public institutions.[4] Also, it is an effective algaecide in swimming pools and industrial water treatment. Soysolv is 100% soybean oil, composed of mixed fatty acid methyl esters. The chemical composition of soysolv is given in Table 1. Its molecular weight and boiling point are 292 g·mol^{-1} and 419 K, respectively.[4] Soysolv is safe, nontoxic, and biodegradable. It is being used as a solvent in many cleaning applications, such as asphalt removal, grease and oil clean up, adhesive removal, welding clean up, and rubber compound cleaning.[4]

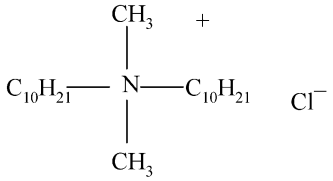

Figure 1. Didecyldimethylammonium chloride.

Table 1. Soysolv Chemical Composition[4]

compound	structure	MW/g·mol^{-1}	wt %
methyl linoleate	$C_{19}H_{34}O_2$	294.5	62.4
methyl oleate	$C_{19}H_{36}O_2$	296.5	22.5
methyl palmitate	$C_{17}H_{34}O_2$	270.5	8.5
methyl linolenate	$C_{19}H_{32}O_2$	292.5	3.2
methyl stearate	$C_{19}H_{38}O_2$	298.5	3.0
methyl palmitoleate	$C_{17}H_{32}O_2$	268.4	0.3
others	na	na	0.1

Solubility data for the system CO_2 + soysolv have received very little attention,[5] but there are phase behavior data for some of the components of soysolv + CO_2, such as CO_2 + methyl linoleate, CO_2 + methyl oleate, and CO_2 + methyl palmitate.[6−8] Stoldt and Brunner measured the solubility of several soybean oil deodorizer distillates (SODDs), obtained from different plants, with CO_2.[9] SODD does not exist in nature, but the refining process of soybean oil produces SODD, which generally comprises mixtures of fatty acid, sterols, hydrocarbons, and vitamins. The composition of SODD is similar to that of soysolv in the sense that both contain fatty acids and ester chains.

We built a phase equilibrium unit capable of generating quantitative solubility and molar volume data for CO_2 in

* To whom correspondence should be addressed. Telephone: (919) 515-5118. Fax: (919) 515-583. E-mail: rgcarbon@pop-in.ncsu.edu.
[†] Current address: Florida Solar Energy Center, 1679 Clearlake Road, Cocoa, FL 32922. E-mail: melbaccouch@fsec.ucf.edu.
[‡] Current address: RTI International, 3040 Cornwallis Road, Research Triangle Park, NC 27709. E-mail: vbondar@rti.org.

10.1021/je020201d CCC: $25.00
Published on Web 10/16/2003

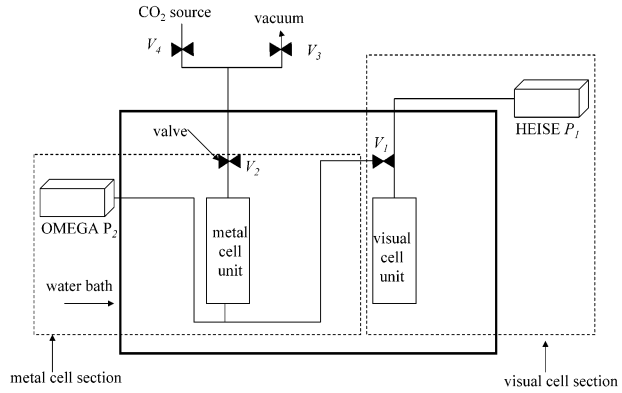

Figure 2. Schematic diagram of the phase equilbrium apparatus: visual cell section, everything to the right of V_1; metal cell section, everything to the left of V_1 and below V_2.

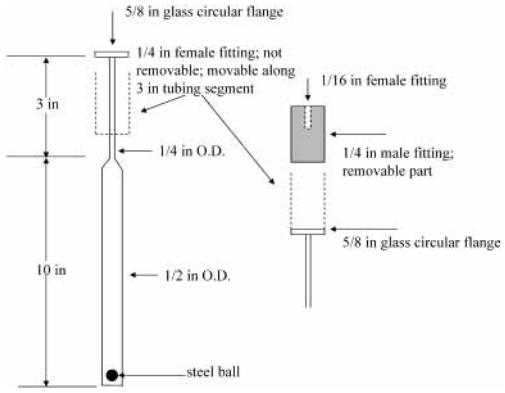

Figure 3. Diagram of the visual cell and the specially designed fitting.

the liquid-phase mixture. As a preliminary step, we tested our solubility measurement capability using a system for which literature data were available at similar conditions to those proposed for the soysolv systems. The phase behavior of CO_2 + nonadecane was selected for comparison because it was well studied and the published data could be used to check the accuracy of our data.[10] We found that our solubility and molar volume data agreed with previous measurements.

In summary, we report the liquid-phase and molar volume data for the binary systems CO_2 + nonadecane at 313.15 K and CO_2 + soysolv at (298.15, 313.15, 323.15, 333.15, and 343.15) K. Also, we report the liquid-phase and molar volume data of the ternary system CO_2 + soysolv + quaternary ammonium chloride surfactant at (298.15, 313.15, and 333.15) K, where the composition of soysolv to the surfactant is 99:1 wt % and 80:20 wt % on a CO_2-free basis. The Appendix summarizes the method used to calculate the mass of CO_2 injected into the equilibrium cell for the stoichiometric measurements.

Experimental Section

Apparatus. The data were generated using a stoichiometric technique, which involves an indirect determination of equilibrium phase compositions. The technique does not require sampling of equilibrium phases; it utilizes mass balances and a volumetrically calibrated cell in determining phase compositions. The setup used in this study is represented schematically in Figure 2. It consists mainly of a visual cell section and a metal cell section. Everything located to the right of valve 1 (V_1) is considered part of the visual cell section. Everything located to the left of V_1 and below V_2 is considered part of the metal cell section. The visual and metal sections are housed in an acrylic water bath. The temperature of the bath is controlled using a heater (Cole Parmer Instrument Co.; Model 12112-10) with an accuracy of ±0.1 °C. The temperature of the content of the system is taken to be the temperature of the liquid bath, which is read directly from the heater's temperature indicator. The $^1/_{16}$ in. tubing located outside the water bath and connecting the pressure indicator to the visual cell is wrapped with a heating tape and heated to the same temperature of the water bath to maintain a uniform temperature throughout the system. Valves V_3 and V_4 are used to apply a vacuum to the system and inject CO_2, respectively.

The Pyrex glass visual equilibrium cell is illustrated in Figure 3. It has a height of 10 in. with a $^1/_2$ in. o.d. body, and it tapers to a 3 in. height and a $^1/_4$ in. o.d. capillary neck. The cell is attached to $^1/_{16}$ in. stainless steel tubing through a specially designed fitting to achieve the required metal-to-glass pressure seal. The specially designed fitting is made from two parts. The first part is a $^1/_4$ in. female fitting located on the capillary neck; it is not removable from the cell body (Figure 3). The second part is a removable fitting containing a $^1/_{16}$ in. female fitting from one end and a $^1/_4$ in. male fitting from the other end. A $^5/_8$ in. glass circular flange is placed on the top of the capillary neck to sandwich the two parts of the fitting together. The visual cell is reliable to pressures of at least 10 MPa. The content of the cell is stirred to achieve phase equilibrium using a steel ball manually actuated up and down in the cell by a magnet.

The pressure inside the visual cell section is measured using a Heise digital pressure transducer (P_1) (model 901-B) having a maximum working pressure of 41 MPa. The digital indicator has a resolution of 0.69 kPa and a rated accuracy of ±6.9 kPa. The pressure inside the metal cell section is measured using an Omega pressure transducer (P_2) (model DP25-S-A). Heise and Omega pressure transducers are calibrated by their manufacturers using instrumentation and standards that are traceable to the U.S. National Institute of Standards and Technology (NIST).

Visual Cell Calibration. A calibration curve is prepared relating the volume of a liquid (hexadecane, MW 226.45 g·mol^{-1}) in the visual cell to its height. The height of the liquid is measured using a cathetometer (Gaertner Scientific Co.; model 2778-A), which allows the volumes to be read in the visual cell to ±0.005 cm^3. The average deviation in the calibration curve is 0.2%. A 1 cm^3 syringe with a 12 in. needle is used to inject a known mass of hexadecane into the visual cell (Mettler Toledo Inc.; model AB-204). The mass of the liquid injected into the visual cell has an accuracy of ±0.1 mg. From the known mass and density of hexadecane (0.773 g·cm^{-3} at 22.4 °C), the injected volume can be calculated, and the corresponding height is measured. In this work, the average mass of liquid injected was within 0.0035 mg. The corresponding average liquid height and volume were within 0.6 cm and 2.69 cm^3.

Assumption. We generated our data assuming that the vapor phase in the visual cell is pure CO_2. Generating multiphase equilibrium data using a stoichiometric technique along with the assumption that the vapor phase is pure CO_2 has been used extensively by Brennecke and co-workers, Khon and co-workers, and Luks and co-workers.[10−16] Chen et al.[16] generated multiphase equilibrium data using the stoichiometric model for the systems

Table 2. Comparison between Vapor Pressures[17] of *n*-Nonadecane and Methyl Oleate (mmHg)

	298 K	313 K	323 K	333 K	343 K
nonadecane	6.0×10^{-5}	3.7×10^{-4}	1.1×10^{-3}	3.1×10^{-3}	7.9×10^{-3}
methyl oleate[a]	6.3×10^{-6}	4.7×10^{-5}	1.6×10^{-4}	4.9×10^{-4}	1.4×10^{-3}

[a] 22.5 wt % in soysolv.

benzene + butane and benzene + propane at temperatures below 273 K. Foreman and Luks[12] measured multiphase equilibrium data for the system *n*-tetradecane + CO_2 in the presence of approximately 1 wt % of methanol at 303 K. In this study, since the composition of ethanol in the soysolv−surfactant−CO_2 mixture is at most 2 wt %, the ethanol partition into the vapor phase is assumed to be negligible.

Table 2 shows the vapor pressures of nonadecane and methyl oleate at several temperatures.[17] The data of Zou and co-workers indicate that at 60 °C the vapor mole fractions of methyl linoleate in CO_2 and methyl oleate in CO_2 are 0.0103 at 91.0 bar and 0.0111 at 92.9 bar, respectively.[7,8] Lockermann reports that the vapor mole fraction of methyl palmitate in the system CO_2 + methyl palmitate at 60 °C and 90 bar is 0.0006.[6] The vapor pressure of nonadecane at 40 °C is similar to that of methyl oleate at 60 °C. So, we might expect their corresponding vapor pressures to be similar.

With the above information as a background, we would like to comment on the effect of the vapor-phase assumption on our data. For each liquid−vapor isotherm, only one liquid injection was utilized. This is an important approach to avoid experimental errors which can result from multiple injections of liquid. Since the height of the liquid mixture increases by adding CO_2, any error associated with the vapor-phase assumption diminishes because the vapor headspace decreases. Injecting a large volume of liquid in order to minimize the vapor headspace causes the meniscus of the liquid mixture to reach the neck of the visual cell before all of the vapor−liquid isotherm is covered. So, there are limits associated with the volume of the liquid injected into the visual cell. As was pointed out in the previous section, the average mass of liquid injected in this study was within 2.69 cm^3. This is roughly 33% of the total volume of the visual cell (9.489 cm^3; Appendix). Our estimation of the required liquid volume allows the collection of all of the solubility data before the meniscus of the liquid mixture reaches the neck of the visual cell, and it diminishes the error associated with the vapor-phase assumption.

Chemicals. CO_2 of minimum purity 99.99% was obtained from National Specialty Gases. Hexadecane (99%) and nonadecane (99.9%) were obtained from Aldrich Chemical Co. Soysolv was obtained from Steyer Farms, Inc. The quaternary ammonium surfactant (BTC-1010-80) was supplied by Sandia National Laboratories.

Procedures. A known mass of the heavy hydrocarbon (i.e. nonadecane) was added to the visual cell using a 12 in. needle syringe. The metal cell section and the vapor space above the liquid in the visual cell section were vacuumed, and CO_2 was added to the metal cell section. Valve V_1 was opened to transfer CO_2 from the metal cell section to the visual cell section. The mass of CO_2 inside the metal cell section before opening V_1 minus the mass of CO_2 inside the metal cell section after opening V_1 was equal to the mass of CO_2 transferred to the visual cell section (Appendix). The steel ball inside the visual cell was manually actuated using an external magnet to achieve equilibrium.

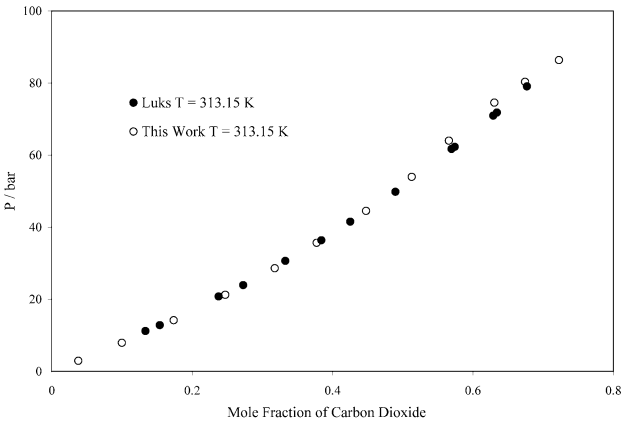

Figure 4. Pressure vs CO_2 liquid-phase mole fraction for the system CO_2 + nonadecane.[10]

Table 3. Liquid-Phase Mole Fraction and Molar Volume of the Mixture as a Function of Pressure for the Liquid−Vapor Isotherm of the CO_2 (1) + *n*-Nonadecane System

T/K	*P*/bar	x_1	molar vol/$cm^3 \cdot mol^{-1}$
313.15	2.93	0.0379	337.9
313.15	7.92	0.0999	319.1
313.15	14.20	0.174	296.3
313.15	21.24	0.247	274.3
313.15	28.61	0.318	253.3
313.15	35.67	0.378	235.5
313.15	44.52	0.448	214.6
313.15	53.95	0.513	196.0
313.15	64.02	0.566	181.6
313.15	74.56	0.631	162.6
313.15	80.34	0.674	148.1
313.15	86.38	0.723	129.9

Since we are assuming that the vapor space above the liquid mixture in the visual cell section is pure CO_2, the density of CO_2 in the vapor space can be calculated from the temperature of the water bath and the Heise pressure indicator. By subtracting the volume of the liquid mixture from the total volume of the visual cell section (calculated in the Appendix), the volume of the vapor space above the liquid phase is obtained. From the density of CO_2 in the vapor space and the volume of the vapor space, the mass of CO_2 in the vapor space is obtained. By subtracting the mass of CO_2 in the vapor space from the total mass of CO_2 injected in the visual cell (calculated in the Appendix), the mass of CO_2 in the liquid phase is obtained. The molar volume of the liquid phase mixture can be calculated be dividing the volume of the liquid phase mixture by the total number of moles (CO_2 and hydrocarbon) in the liquid mixture.

Liquid-phase and molar volume data for CO_2 + nonadecane at 313.15 K are presented in Table 3. Figures 4 and 5 show that our data for the system CO_2 + nonadecane agree well with those reported by Luks and co-workers[10] at 313.05 K. Table 4 and Figure 6 contain liquid-phase and molar volume data for the system CO_2 + soysolv at (298.15, 313.15, 323.15, 333.15, and 343.15) K. Tables 5 and 6 present liquid-phase and molar volume data for the systems CO_2 + 99:1 and 80:20 wt % soysolv−quaternary ammonium surfactant at (298.15, 313.15, and 333.15) K. The corresponding solubility plots are given in Figures 7 and 8. The presented data show that the liquid-phase mixtures are stable and homogeneous under the operating conditions (i.e. no surfactant precipitation or separate phase formation). Figure 9 shows the pressure as a function of the mixture liquid-phase molar volume for the systems

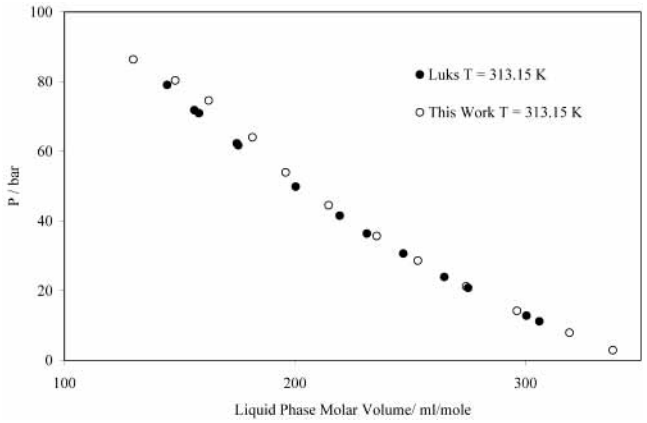

Figure 5. Pressure vs mixture liquid-phase molar volume for the system CO_2 + nonadecane.[10]

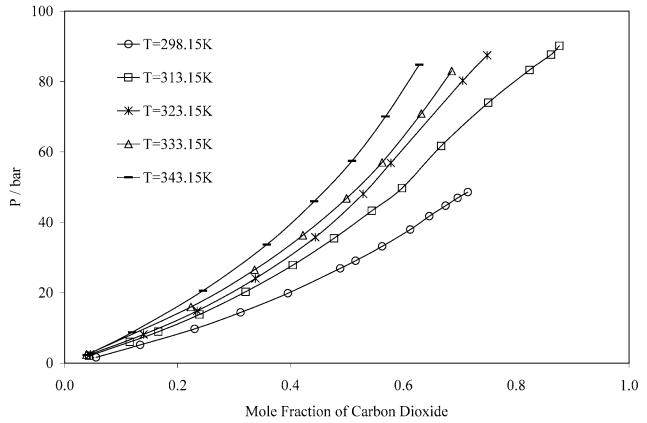

Figure 6. Pressure vs CO_2 liquid-phase mole fraction for the system CO_2 + soysolv.

Table 4. Liquid-Phase Mole Fraction and Molar Volume of the Mixture as a Function of Pressure for the Liquid−Vapor Isotherms of the CO_2 (1) + Soysolv System

T	P		mol vol	T	P		mol vol
K	bar	x_1	$cm^3 \cdot mol^{-1}$	K	bar	x_1	$cm^3 \cdot mol^{-1}$
298.15	1.62	0.0557	311.4	323.15	2.468	0.045	327.3
298.15	5.16	0.134	288.2	323.15	8.129	0.140	297.6
298.15	9.70	0.230	262.5	323.15	14.851	0.235	271.2
298.15	14.40	0.312	239.8	323.15	24.035	0.338	241.9
298.15	19.84	0.396	215.8	323.15	35.74	0.444	211.8
298.15	26.92	0.488	190.0	323.15	48.06	0.529	189.0
298.15	29.05	0.515	182.1	323.15	56.87	0.578	176.3
298.15	33.17	0.563	168.8	323.15	80.27	0.706	143.2
298.15	37.94	0.612	154.8	323.15	87.47	0.748	129.4
298.15	41.74	0.646	146.3				
298.15	44.71	0.675	138.1	333.15	2.37	0.0387	322.0
298.15	46.93	0.696	132.0	333.15	8.37	0.124	278.3
298.15	48.58	0.714	126.7	333.15	15.92	0.224	268.6
				333.15	26.52	0.337	236.6
313.15	2.06	0.044	326.3	333.15	36.34	0.422	212.6
313.15	6.01	0.116	305.4	333.15	46.79	0.499	190.9
313.15	8.91	0.166	290.5	333.15	57.03	0.563	172.9
313.15	13.82	0.239	269.3	333.15	70.89	0.632	154.1
313.15	20.25	0.321	245.2	333.15	82.98	0.686	139.0
313.15	27.84	0.404	220.2				
313.15	35.44	0.477	200.1	343.15	2.23	0.0393	325.4
313.15	43.26	0.544	181.1	343.15	8.73	0.120	303.2
313.15	49.72	0.598	165.7	343.15	20.54	0.245	266.8
313.15	61.72	0.667	148.4	343.15	33.67	0.358	233.9
313.15	74.01	0.751	124.2	343.15	45.96	0.442	210.6
313.15	83.30	0.824	99.2	343.15	57.41	0.509	191.5
313.15	87.66	0.862	83.1	343.15	70.06	0.568	175.0
313.15	90.17	0.877	76.0	343.15	84.78	0.628	159.5

CO_2 + soysolv, CO_2 + 99:1 wt % soysolv−BTC, and CO_2 + 80:20 wt % soysolv−BTC at (298.15 and 333.15) K. The figures show that the addition of the BTC surfactant enhances the solubility of the CO_2 in the liquid mixture.

Table 5. Liquid-Phase Mole Fraction and Molar Volume of the Mixture as a Function of Pressure for Liquid−Vapor Isotherms of CO_2 (1) + a 99:1 wt % Mixture of Soysolv + BTC-1010-80[a]

T	P		mol vol	T	P		mol vol
K	bar	x_1	$cm^3 \cdot mol^{-1}$	K	bar	x_1	$cm^3 \cdot mol^{-1}$
298.15	2.01	0.0477	318.5	313.15	50.06	0.615	158.5
298.15	5.14	0.121	297.7	313.15	56.41	0.659	145.9
298.15	9.78	0.217	270.8	313.15	61.40	0.694	135.4
298.15	14.92	0.306	245.5	313.15	69.17	0.740	123.1
298.15	20.87	0.399	218.3	313.15	76.42	0.789	107.8
298.15	26.23	0.469	198.3	313.15	83.22	0.835	88.4
298.15	31.96	0.540	178.5	313.15	87.38	0.862	76.1
298.15	37.74	0.603	160.1				
298.15	41.58	0.641	149.4	333.15	2.88	0.0478	328.9
298.15	43.79	0.661	143.6	333.15	8.29	0.123	307.3
298.15	47.13	0.691	135.1	333.15	16.28	0.228	275.7
298.15	49.59	0.718	127.1	333.15	25.15	0.323	247.7
				333.15	34.60	0.408	222.3
313.15	2.30	0.048	324.9	333.15	43.64	0.475	202.5
313.15	7.47	0.144	296.2	333.15	51.76	0.530	186.5
313.15	16.49	0.293	251.6	333.15	66.13	0.606	165.3
313.15	25.75	0.403	220.1	333.15	79.65	0.666	148.0
313.15	33.39	0.479	197.5	333.15	87.40	0.691	132.0
313.15	40.38	0.544	178.7				

[a] BTC-1010-80 is didecyldimethylammonium chloride.

Conclusions

A volumetrically calibrated visual cell was used to measure the solubility of CO_2 in soysolv and in a soysolv + quaternary ammonium chloride surfactant mixture. The liquid-phase compositions are determined by stoichiometry assuming that the vapor phase is pure CO_2. The challenge of accurately calibrating the total volume of the visual cell and calculating the mass of CO_2 has been overcome by utilizing a dual-volume technique. The accuracy of our techniques is verified by successfully reproducing solubility data for the system CO_2 + nonadecane.

The generated data demonstrate the capability of CO_2 modified soysolv to be an effective transport solvent for the quaternary ammonium chloride surfactant. The CO_2−BTC surfactant mixture is not miscible, but soysolv is miscible in the BTC surfactant. Figure 7 shows that CO_2 is soluble in soysolv under 100 bar. This work demonstrates a heterogeneous separating process comprised of three steps.[18] First, two immiscible phases are formed containing CO_2 in the first phase and the insoluble surfactant in the second phase. Second, soysolv is added to the surfactant to produce a completely soluble mixture in the second phase. Third, CO_2 is added to the second phase, in which CO_2 becomes soluble in the soysolv−surfactant mixture. Figures 8 and 9 show that CO_2 is soluble in the soysolv−surfactant mixture and as a result CO_2 can effectively extract the BTC surfactant. Also, the figures show that the solubility of CO_2 in the liquid phase of the mixture increases as the mass percentage of the surfactant in soysolv increases. This is indicated by the increase in the molar volume of the liquid mixture as the mass of the BTC surfactant increases in the mixture. Comparing the pressure ranges of Figures 7−9, the solubilities of the isothermal binary and ternary mixtures are within the same range.

It should be noted that a second liquid-phase rich in CO_2 was observed at 25 °C and 62 bar. Also, data were not

Table 6. Liquid-Phase Mole Fraction and Molar Volume of the Mixture as a Function of Pressure for Liquid−Vapor Isotherms of CO_2 (1) + a 80:20 wt % Mixture of Soysolv + BTC-1010-80[a]

T	P		mol vol	T	P		mol vol
K	bar	x_1	$cm^3 \cdot mol^{-1}$	K	bar	x_1	$cm^3 \cdot mol^{-1}$
298.15	1.88	0.0441	333.4	313.15	79.33	0.795	105.6
298.15	4.65	0.105	314.0	313.15	82.98	0.830	91.5
298.15	9.68	0.206	282.3	313.15	85.74	0.851	82.9
298.15	16.12	0.316	249.0	313.15	87.51	0.864	77.0
298.15	26.40	0.459	205.3	313.15	89.01	0.872	72.8
298.15	38.06	0.581	169.6				
298.15	44.34	0.641	152.3	333.15	3.41	0.0499	340.9
298.15	48.10	0.681	140.1	333.15	8.96	0.119	217.0
298.15	50.68	0.704	133.5	333.15	15.42	0.193	292.6
				333.15	22.61	0.263	270.6
313.15	3.48	0.0649	331.4	333.15	29.66	0.324	250.9
313.15	7.48	0.134	309.8	333.15	38.20	0.393	228.9
313.15	11.62	0.199	289.1	333.15	44.00	0.435	215.5
313.15	16.95	0.271	266.4	333.15	50.46	0.479	202.1
313.15	21.69	0.333	247.5	333.15	57.51	0.521	188.9
313.15	26.37	0.386	231.2	333.15	64.31	0.559	177.4
313.15	31.41	0.439	214.7	333.15	72.15	0.599	165.9
313.15	37.85	0.590	197.2	333.15	76.68	0.621	158.9
313.15	43.11	0.540	184.2	333.15	82.11	0.648	150.5
313.15	49.72	0.592	168.4	333.15	87.62	0.679	140.4
313.15	54.72	0.626	158.6	333.15	91.34	0.695	135.1
313.15	59.00	0.657	148.7	333.15	93.72	0.704	132.3

[a] BTC-1010-80 is didecyldimethylammonium chloride.

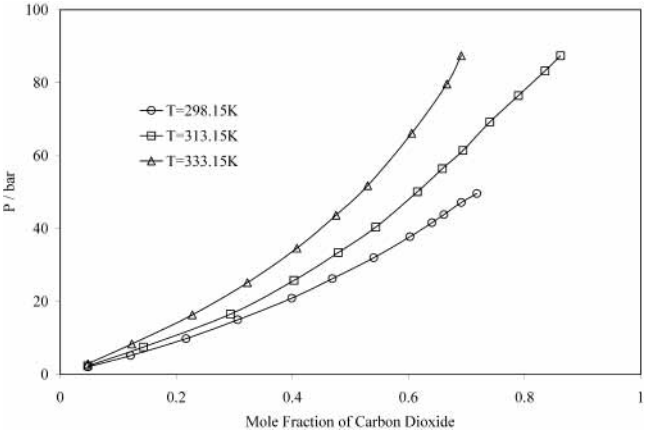

Figure 7. Pressure vs CO_2 liquid-phase mole fraction for the system CO_2 + 99:1 wt % soysolv−BTC.

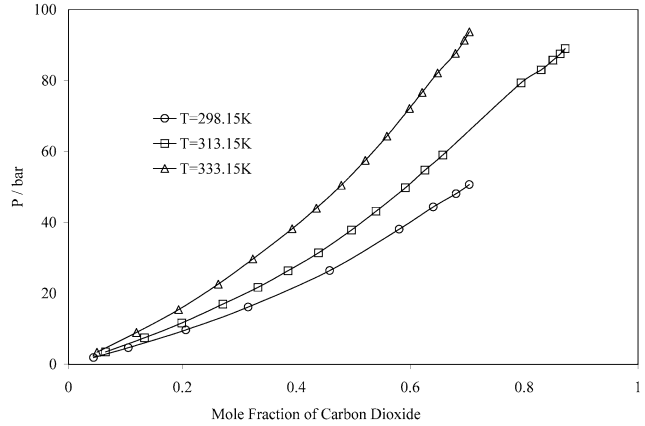

Figure 8. Pressure vs CO_2 liquid-phase mole fraction for the system CO_2 + 80:20 wt % soysolv−BTC.

generated beyond 90 bar due to the pressure limit of the apparatus (100 bar). That motivates us to suggest the use of a different stoichiometric apparatus with a higher pressure limit in order to have the capability to generate

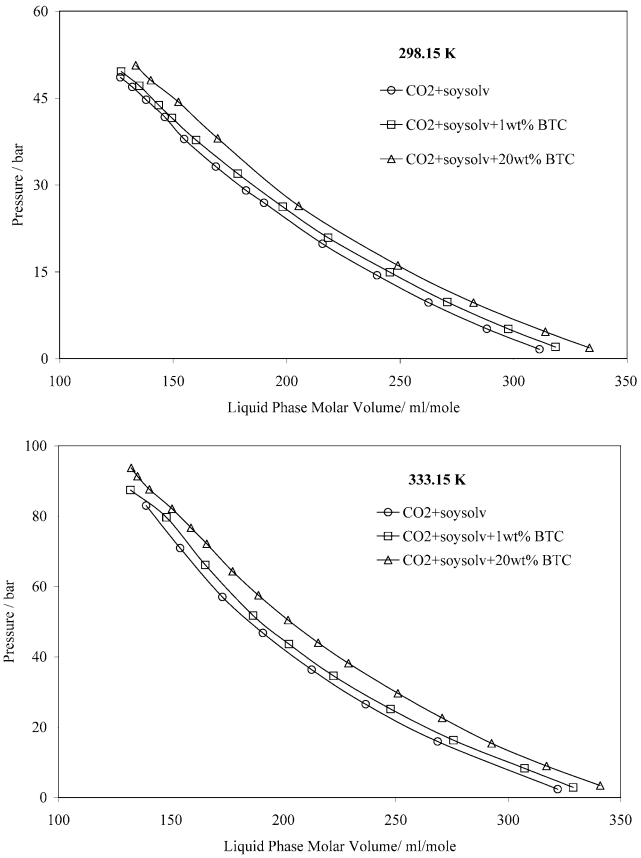

Figure 9. Pressure vs mixture liquid-phase molar volume for the systems CO_2 + 99:1 and 80:20 wt % soysolv−BTC at (A) 298.15 K and (B) 333.15 K.

solubility data for multiple liquid phases at a larger range of temperatures and pressures.[19,20]

Acknowledgment

We would like to thank Professors Joan Brennecke and James Kohn from the University of Notre Dame for their assistance in building the equilibrium visual cell.

Appendix

Phase equilibrium experiments require precise and expensive equipment for measurements of pressure, temperature, and volume. Luks and co-workers[10−13] and Kohn and co-workers[14] used Ruska pumps (Ruska Instrument Co.) to calculate the mass of CO_2 injected into the equilibrium cells. As an alternative technique, we calculated the mass of CO_2 in the visual cell section by utilizing a dual volume system, which was considered by a number of investigators for the measurement of gas sorption in polymers.[21−25] The mass of CO_2 injected into the visual cell section is equal to the difference in the mass of CO_2 inside the metal cell section, calculated from the gas law, before and after opening valve V_1. The following is a procedure for calculating the total volumes of the metal cell section and visual cell section.

The experimental apparatus was vacuum pumped, and the water bath was heated to 40 °C. Valve V_1 was closed and the visual cell section was pressurized with nitrogen. Then, valve V_1 was opened, letting nitrogen expand into the metal cell section. Since the total mass of nitrogen before and after opening V_1 is the same, mass balance

equations can be expressed as follows.

$$n(\text{before expansion}) = n(\text{after expansion}) \quad (1)$$

$$\frac{P_i V_G}{Z_i R T} = \frac{P_f (V_G + V_M)}{Z_f R T} \quad (2)$$

where n is the number of moles of nitrogen, and V_G and V_M are the total volumes of the visual cell section and metal cell section, respectively. P_i is the initial pressure in the visual cell section before expansion, P_f is the final pressure in the visual and metal cell sections after expansion, R is the universal gas constant, and T is the temperature (40 °C). Z_i and Z_f are the compressibility factors of nitrogen at pressures P_i and P_f, respectively.[26] The volume ratio of the metal and visual sections can be expressed by arranging eq 2 as

$$\frac{V_M}{V_G} = \frac{P_i Z_f}{P_f Z_i} - 1 = Q_1 \quad (3)$$

The constant Q_1 was determined on the basis of 10 parallel expansion experiments at 40 °C and different pressures while placing the metal cell section under a vacuum prior to each pressure load. The average Q_1 value was equal to 0.7658 with a 0.006 standard deviation.

A similar set of expansion measurements was conducted with stainless steel spheres of a known volume V_B inside the metal cell. The volume of the spheres was determined by a picnometric technique and was found to be 2.249 cm^3 with a 0.018 standard deviation. The calibration procedure was the same as that described above, and eq 2 can be expressed as

$$\frac{V_M^*}{V_G} = \frac{V_M - V_B}{V_G} = \frac{P_i Z_f}{P_f Z_i} - 1 = Q_2 \quad (4)$$

where V_M^* is the volume of the metal cell section minus the volume of the spheres. The constant Q_2 was found to be equal to 0.5843 with a 0.003 standard deviation. The constant Q_2 was based on over 20 different pressure loads of nitrogen at 40 °C, while placing the metal cell section under a vacuum prior to each expansion. The final expressions for the visual cell section and the metal cell section are given as follows.

$$V_G = \frac{V_B}{Q_1 - Q_2} \quad (5)$$

$$V_M = V_G Q_1 \quad (6)$$

The volumes of the visual cell section V_G and the metal cell section V_M were found to be 9.489 cm^3 and 12.391 cm^3, respectively. A blank nitrogen experiment based on over 50 runs was conducted to verify the accuracy of the volumes V_G and V_M. The absolute percentage error between the moles of nitrogen removed from the metal cell section and the corresponding moles transferred to the visual cell section was within 0.28%.

Literature Cited

(1) McHugh, M.; Krukonis, V. *Supercritical Fluid Extraction*, 2nd ed.; Butterworth-Heinemann: Boston, MA, 1994.

(2) Canelas, D.; DeSimone, J. Polymerizations in Liquid and Supercritical Carbon Dioxide. *Adv. Polym. Sci.* **1997**, *133*, 103−140.

(3) Wang, J.; Even, B. Personal Communication. Sandia National Laboratories, Livermore, CA 94550.

(4) Styer Farms, Inc. Technical Communications, Tiffin, OH 44883.

(5) Fogg, P. *Solubility Data Series—Carbon Dioxide in Non-Aqueous Solvents at Pressures Less Than 200 Kpa*; Pergamon Press: Oxford, 1992; Vol. 50, pp 444−445.

(6) Lockermann, A. C. High-Pressure Phase Equilibria and Densities of the Binary Mixtures Carbon Dioxide-Oleic Acid, Carbon Dioxide-Methyl Myristate, and Carbon Dioxide-Methyl Palmitate and the Ternary Mixture Carbon Dioxide-Methyl Myristate-Methyl Palmitate. *Chem. Eng. Process.* **1994**, *33*, 171−187.

(7) Zou, M.; Yu, R. Z.; Rizvi, H. S.; Zollweg, A. J. Fluid-Liquid Equilibria of Ternary Systems of Fatty Acids and Fatty Esters in Supercritical CO_2. *J. Supercrit. Fluids* **1990**, *3*, 85−90.

(8) Zou, M.; Yu, R. Z.; Kashulines, S. S.; Rizvi, H. S.; Zollweg, A. J. Fluid-Liquid-Phase Equilibria of Fatty Acids and Fatty Acid Methyl Esters in Supercritical CO_2. *J. Supercrit. Fluids* **1990**, *3*, 23−28.

(9) Stoldt, J.; Brunner, G. Phase Equilibrium Measurements in Complex Systems of Fats, Fat Compounds in Supercritical Carbon Dioxide. *Fluid Phase Equilib.* **1998**, *146*, 269−295.

(10) Fall, D.; Fall, J.; Luks, K. Liquid−Liquid-Vapor Immiscibility limits in Carbon Dioxide + n-Paraffin Mixtures. *J. Chem. Eng. Data* **1985**, *30*, 82−88.

(11) Fall, D.; Luks, K. Phase Equilibria Behavior of the Systems Carbon Dioxide + n-Dotriacontane and Carbon Dioxide + n-Docosane. *J. Chem. Eng. Data* **1984**, *29*, 413−417.

(12) Foreman, C.; Luks, K. Partial Miscibility Behavior of the Ternary Mixture Carbon Dioxide + n-Tetradecane + Methanol. *J. Chem. Eng. Data* **2000**, *45*, 334−337.

(13) Lam, D.; Luks, K. Multiphase Equilibrium Behavior of the Mixture Ethane + Methanol + 1-Decanol. *J. Chem. Eng. Data* **1991**, *36*, 307−311.

(14) Tarantino, D.; Kohn, J.; Brennecke, J. Phase Equilibrium Behavior of the Carbon Dioxide + Benzophenone Binary System. *J. Chem. Eng. Data* **1994**, *39*, 158−160.

(15) Tiffin, D.; Luks, K. Solid Hydrocarbon Solubility in Liquid Methane-Ethane Mixtures along Three-Phase Solid−Liquid-Vapor Loci. *J. Chem. Eng. Data* **1979**, *24*, 306−310.

(16) Chen, W. L.; Luks, K.; Kohn, J. Three-Phase Solid−Liquid-Vapor Equilibria of the Binary Hydrocarbon Systems Propane-Benzene, Propane Cyclohexane, *n*-Butane-Benzene, *n*-Butane-Cyclohexane, *n*-Butane-*n*-Decane, and *n*-Butane-n-Dodecane. *J. Chem. Eng. Data* **1981**, *26*, 310−312.

(17) Yaws, L. C. *Chemical Properties Handbook*; McGraw-Hill: New York, 1999.

(18) Romack, T. J.; McClain, J. B.; Stewart, G. M.; Givens, R. D. Carbon Dioxide Cleaning and Separation Systems. Patent US-6120613, 2000.

(19) Khan, V. A. Solubility of Gases in Molten Polymers at High Pressures. Dissertation, Wayne State University, 1998.

(20) Stradi, G. B. Measurement and Modeling of the Phase Behavior of High-Pressure-Reaction Mixtures and the Computation of Mixture Critical Points. Dissertation, University of Notre Dame, 2000.

(21) Bondar, V.; Freeman, B. Sorption of Gases and Vapors in an Amorphous Glassy Perfluorodioxole Copolymer. *Macromolecules* **1999**, *32*, 6163−6171.

(22) Koros, J. W.; Paul, R. D. Design Considerations for Measurements of Gas Sorption in Polymers by Pressure Decay. *J. Polym. Sci.* **1976**, *14*, 1903−1907.

(23) Sada, E.; Kumazawa, H.; Xu, P. Sorption and diffusion of carbon dioxide in polyimide films. *J. Appl. Polym. Sci.* **1988**, *35*, 1497−1509.

(24) Sanders, E. S.; Koros, W. J.; Hopfenberg, H. B.; Stannett, V. T. Pure and mixed gas sorption of carbon dioxide and ethylene in poly(methyl methacrylate). *J. Membr. Sci.* **1984**, *18*, 53−74.

(25) Vieth, R. W.; Tam, M. P.; Michaels, S. A. Dual Sorption Mechanisms in Glassy Polystyrene. *J. Colloid Interface Sci.* **1966**, *22*, 360−370.

(26) Ely, J. F.; Magee, J. W.; Haynes, W. M. *Thermophysical Properties for Special High CO_2 Content Mixtures*; U.S. National Institute of Standards and Technology (NIST) Research Report RR-110; Gas Processors Association: Tulsa, OK, p 987.

Received for review November 18, 2002. Accepted July 11, 2003. This material is based upon work supported by the STC Program of the National Science Foundation under Agreement No. CHE-9876674.

JE020201D